Journal of Pharmacology and Toxicology

ISSN 1816-496X

Academic Journals Inc.

www.academicjournals.com

Journal of Pharmacology and Toxicology 2 (7): 599-609, 2007
ISSN 1816-496X

Molecular Modelling Analyses of the Metabolism of Clofarabine

Fazlul Huq
Discipline of Biomedical Science, School of Medical Sciences, Faculty of Medicine, Cumberland Campus, C42, The University of Sydney, Lidcombe, NSW, Australia

Abstract: Clofarabine (CLF) is a new purine nucleoside antimetabolite developed for the treatment of solid and hematologic tumours. In this study molecular modelling analyses based on molecular mechanics, semi-empirical (PM3) and DFT (at B3LYP/6-31G* level) calculations have been carried out to gain information on the relative toxicity of CLF and its metabolites. The study shows that CLF and its metabolites have large LUMO-HOMO energy differences of the order 5.3 eV from DFT calculations, indicating that CLF and all its metabolites would be kinetically inert. The molecular surfaces of CLF and all its metabolites are found to possess significant amounts of electron-rich (yellow and red) and neutral (green) regions so that the compounds may be subject to electrophilic and lyophilic attacks. However, the molecular surfaces do not appear to abound in electron-deficient (blue) regions (although the presence may be significant in the case of CLF, 2CAD and CLFDP) so that the compounds generally may not react to any significant extent with cellular nucleophiles such as the reduced form of glutathione and nucleobases in DNA. This means that other factors besides glutathione depletion and DNA damage may be playing key role in toxicity of CLF and its metabolites.

Key words: Clofarabine, hematologic tumours, nucleoside prodrug, molecular modelling

INTRODUCTION

Clofarabine (2-chloro-2'-fluoro-deoxy-9-β-D-arabinofuranosyladenine; CLF) is a new purine nucleoside antimetabolite drug developed for the treatment of solid and hematologic tumours (Beonate *et al*., 2005; Hegde and Schmidt, 2006). The presence of a fluorine atom in the C-2' position renders CLF less susceptible to phosphorolytic cleavage of the glycosidic bond and inactivation by purine nucleoside phosphorylases. In addition, the presence of C-2' fluoro group in CLF improves its acid stability as compared to its predecessors such as cladribine and fludarabine. CLF is found to be cytotoxic to rapidly proliferating and quiescent cancer cell types *in vitro* including CEM, K562, Hep2, L1210 leukaemia, p388 leukaemia and colon 36 (Plunkett and Gandhi, 2001). In both phase 1 and phase 2 studies, CLF has shown impressive clinical activity as a single agent against leukaemia without causing neurotoxicity (Faderi *et al*., 2005). The maximum tolerated dose (MTD) of CLF in adult patients with solid tumours is 2 mg m^{-2} with Dose Limiting Toxicity (DLT) being myelosuppression (Beonate *et al*., 2005).

CLF is a prodrug that must be metabolized within the cell to clofarabine monophosphate (CLFMP), clofarabine diphosphate (CLFDP) and finally to clofarabine triphosphate (CLFTP) for activity to be observed (Beonate *et al*., 2005). It is postulated that the active metabolite CLFTP has multiple mechanisms of action including (1) inhibition of DNA polymerase α, (2) inhibition of ribonucleotide reductase and (3) disruption of mitochondrial function through release of cytochrome c and proapoptotic proteins. The additive effect of these parallel events leads to programmed cell death due to the depletion of intracellular deoxynucleotide triphosphate pools, inhibition of DNA strands elongation during synthesis and release of proapototic mitochondrial factors in both actively dividing

and quiescent tumour cells (Parker *et al*., 1991; Xie and Plunkett, 1996; Beonate *et al*., 2005). Other metabolites of CLF are carboxyclofrabine (CCLF), two clofarabine glucuronides (CLFG1 and CLFG2), 2-chloroadenine (2CAD), 6-ketoclofarabine (6KCLF) and two clofarabine sulfates (CLFS1 and CLFS2). Figure 1 summarizes the metabolic pathways for CLF in humans.

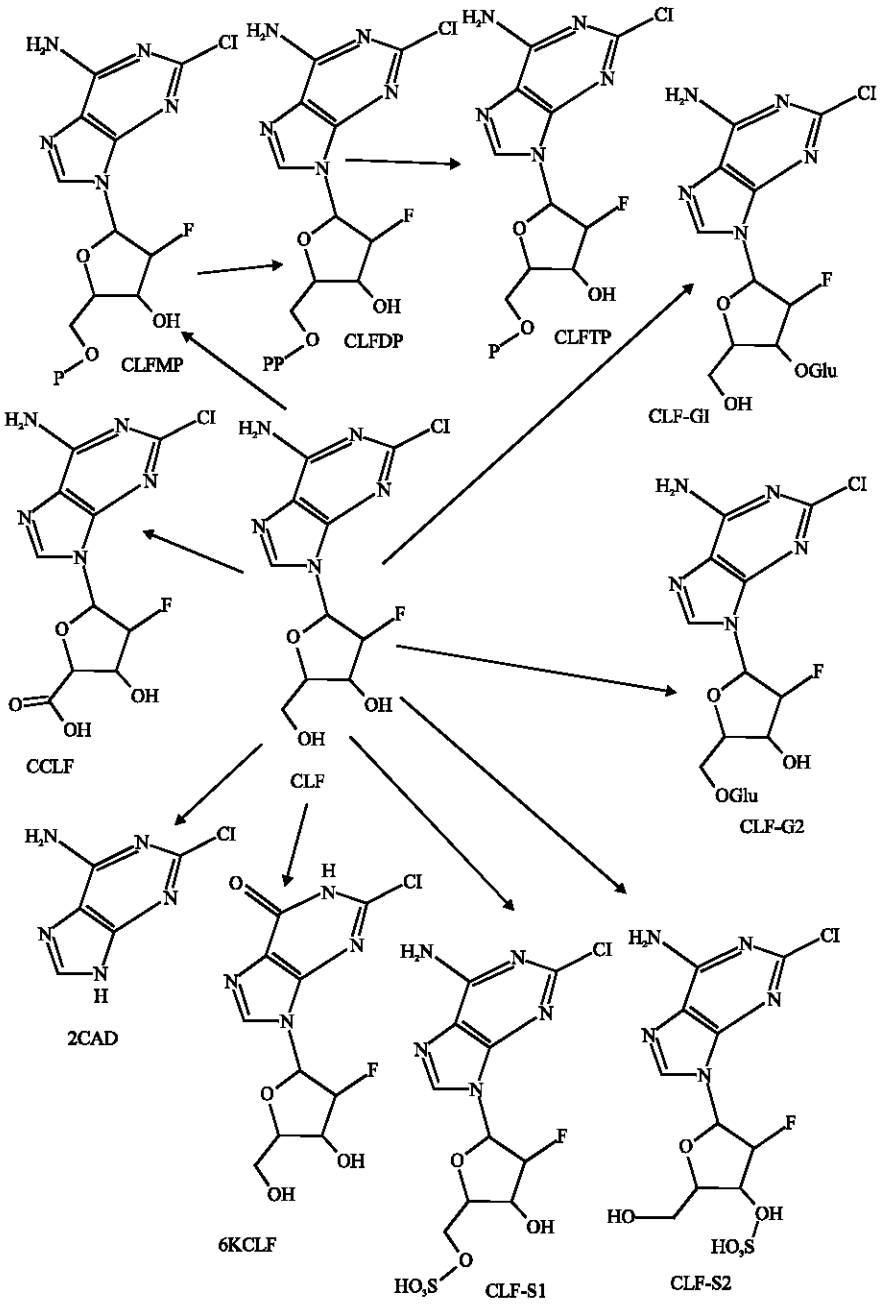

Fig. 1: Metabolic pathways for CLF in humans (Beonate *et al*., 2005)

In this study, molecular modelling analyses have been carried out using the program Spartan '02 (Spartan, 2002) of CLF and its metabolites with the aim of providing a better understanding of their relative toxicity. Previous studies have shown that xenobiotics and their metabolites which are kinetically labile and abound in electron-deficient regions on the molecular surface tend to induce cellular toxicity due to glutathione depletion and cause DNA damage due to oxidation of nucleobases in DNA (Huq, 2006a, b). The research was carried out in the Discipline of Biomedical Science, School of Medical Sciences, The University of Sydney during February to April 2007.

MATERIALS AND METHODS

Molecular modelling calculations carried out in this study are described as follows.

Computational Methods

The geometries of CLF and its metabolites have been optimised based on molecular mechanics, semi-empirical and DFT (Density functional theory) calculations, using the molecular modelling program Spartan '02. Molecular mechanics calculations were carried out using MMFF force field. Semi-empirical calculations were carried out using the routine PM3. DFT calculations were carried at B3LYP/6-31G* level. In optimization calculations, a RMS gradient of 0.001 was set as the terminating condition. For the optimised structures, single point calculations were carried out to give heat of formation, enthalpy, entropy, free energy, dipole moment, solvation energy, energies for HOMO (Highes occupied molecular orbital) and LUMO (Lowest unoccupied molecular orbital). The order of calculations: molecular mechanics followed by semi-empirical followed by DFT ensured that the structure was not embedded in a local minimum. To further check whether the global minimum was reached, some calculations were carried out with improvable structures. It was found that when the stated order was followed, structure corresponding to the global minimum or close to that could ultimately be reached in all cases. Although RMS gradient of 0.001 may not be sufficiently low for vibrational analysis, it is believed to be sufficient for calculations associated with electronic energy levels (Huq and Alsheri, 2006).

RESULTS AND DISCUSSION

Table 1 gives the total energy, heat of formation as per PM3 calculation, enthalpy, entropy, free energy, surface area, volume, dipole moment and energies of HOMO and LUMO as per both PM3 and DFT calculations for CLF and its metabolites. Figure 2-12 give the regions of negative electrostatic potential (greyish-white envelopes) in (a), HOMOs (where red indicates HOMOs with high electron density) in (b), LUMOs in (c) and density of electrostatic potential on the molecular surface (where red indicates negative, blue indicates positive and green indicates neutral) in (d) as applied to optimised structures of CLF, CCLF, 2CAD, CLFG1, CLFG2, 6KCLF, CLFMP, CLFDP, CLFTP, CLFS1 and CLFS2.

The LUMO-HOMO energy differences for CLF, CCLF, 2CAD, CLFG1, CLFG2, 6KCLF, CLFMP, CLFDP, CLFTP, CLFS1 and CLFS2 from DFT calculations are found to be large (of the order of 5.3 eV from DFT calculations) (Table 1), indicating that the compounds would be kinetically inert.

The solvation energies of CLF, CCLF, 2CAD, CLFG1, CLFG2, 6KCLF, CLFS1 and CLFS2 obtained from PM3 calculations are found to range from -21.4 to -37.1 kcal mol^{-1}, indicating that the compounds would have moderate to high solubility in water. The solvation energies of CLFMP, CLFDP and CLFTP could not be calculated as the program was not parametrized for phosphorus.

Table 1: Calculated thermodynamic and other parameters of CLF and its metabolites (DM stands for dipole moment)

Molecule	Calculation type	1	2	3	4	5	6	7	8	9	10	11	12
CLF	PM3		-119.97	637.80	597.09	459.78	-21.38	280.39	250.00	4.6	-8.86	-0.58	8.28
	DFT	-1447.13		639.31	596.43	461.57	-20.14	273.12	246.82	6.0	-6.11	-0.74	5.37
CCLF	PM3		-159.32	597.70	608.34	412.33	-24.36	282.45	252.22	2.5	-9.08	-0.83	8.25
	DFT	-1521.17		598.92	607.26	417.96	-22.75	274.28	248.88	5.9	-6.34	-0.96	5.38
2CAD	PM3		48.56	288.85	384.67	174.16	-19.68	161.56	137.82	2.9	-8.89	-0.61	8.28
	DFT	-926.92		293.31	382.94	179.14	-17.94	159.85	136.08	4.3	-6.18	-0.77	5.41
CLFG1	PM3		-413.23	294.97	381.57	181.26	-36.39	432.38	397.35	3.7	-8.95	-0.69	8.26
	DFT	-2207.13		296.64	380.69	183.19	-35.37	412.37	391.66	7.8	-6.11	-0.74	5.37
CLFG2	PM3		-415.40	1085.59	831.91	837.56	-37.07	426.76	396.61	5.8	-8.88	-0.61	8.27
	DFT	-2207.13		1087.64	830.67	840.10	-35.42	412.49	391.69	7.8	-6.11	-0.75	5.36
6KCLF	PM3		-163.55	603.95	602.12	424.43	-20.92	276.09	247.10	5.6	-9.13	-0.83	8.30
	DFT	-1467.00		605.75	600.67	426.75	-19.48	268.71	244.16	6.0	-6.34	-1.10	5.24
CLFMP	PM3		-327.30	711.71	727.12	494.92		339.55	296.46	5.2	-8.87	-0.59	8.28
	DFT	-2014.68		712.92	726.01	496.57		322.21	291.03	6.0	-6.06	-0.68	5.38
CLFDP	PM3		-542.93	787.80	811.67	545.70		391.59	341.75	8.1	-8.70	-0.70	8.00
	DFT	-2582.58		789.62	810.31	548.14		379.71	337.00	8.1	-5.98	-0.58	5.40
CLFTP	PM3		-758.98	863.72	904.81	593.95		445.06	387.03	10.1	-8.67	-0.87	7.80
	DFT	-3150.30		865.31	903.57	596.05		425.02	380.01	9.1	-6.03	-0.70	5.33
CLFS1	PM3		-246.53	680.68	708.10	469.56	-34.22	333.25	291.80	4.1	-8.93	-0.66	8.27
	DFT	-2070.93		682.29	706.81	471.66	-33.04	325.19	288.72	6.4	-6.20	-0.81	5.39
CLFS2	PM3		-246.04	681.27	703.53	471.53	-33.14	333.72	291.90	3.1	-8.85	-0.69	8.16
	DFT	-2070.92		683.69	702.86	474.24	-32.08	324.79	288.86	3.8	-6.95	-0.98	5.97

1 = Total energy (kcal mol^{-1}/atomic unit*), 2 = Heat of formation (kcal mol^{-1}), 3 = Enthalpy (kcal $mol^{-1}K^{-1}$), 4 = Entropy (cal mol^{-1} K^{-1}), 5 = Free energy (kcal mol^{-1}), 6 = Solvation energy (kcal mol^{-1}), 7 = Area ($Å^2$), 8 = Volume ($Å^3$), 9 = DM (debye), 10 = HOMO (eV), 11 = LUMO (eV) and 12 = LUMO-HOMO (eV), *: in atomic units from DFT calculations

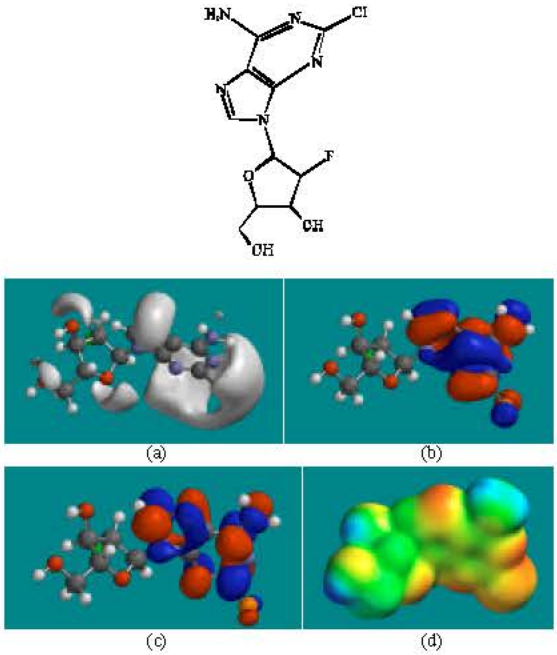

Fig. 2: Structure of CLF giving in: (a) the electrostatic potential (greyish envelope denotes negative electrostatic potential), (b) the HOMOs, (where red indicates HOMOs with high electron density), (c) the LUMOs (where blue indicates LUMOs) and in (d) density of electrostatic potential on the molecular surface (where red indicates negative, blue indicates positive and green indicates neutral)

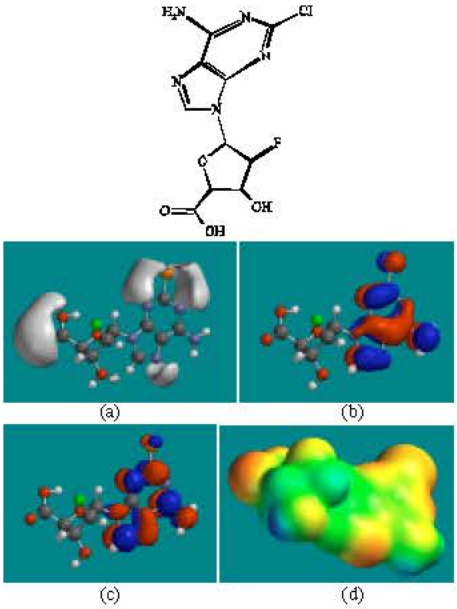

Fig. 3: Structure of CCLF giving in: (a) the electrostatic potential (greyish envelope denotes negative electrostatic potential), (b) the HOMOs, (where red indicates HOMOs with high electron density), (c) the LUMOs (where blue indicates LUMOs) and in (d) density of electrostatic potential on the molecular surface (where red indicates negative, blue indicates positive and green indicates neutral)

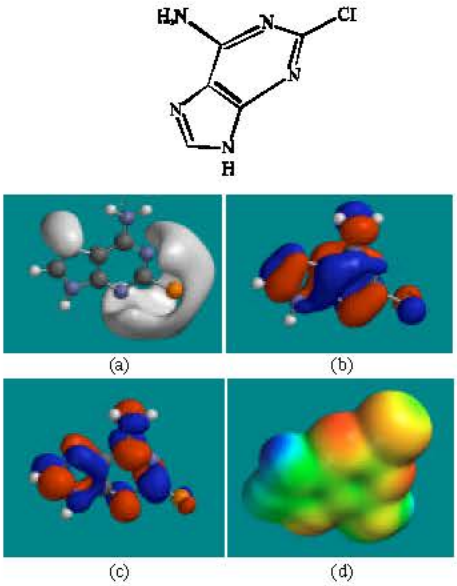

Fig. 4: Structure of 2CAD giving in: (a) the electrostatic potential (greyish envelope denotes negative electrostatic potential), (b) the HOMOs, (where red indicates HOMOs with high electron density), (c) the LUMOs (where blue indicates LUMOs) and in (d) density of electrostatic potential on the molecular surface (where red indicates negative, blue indicates positive and green indicates neutral)

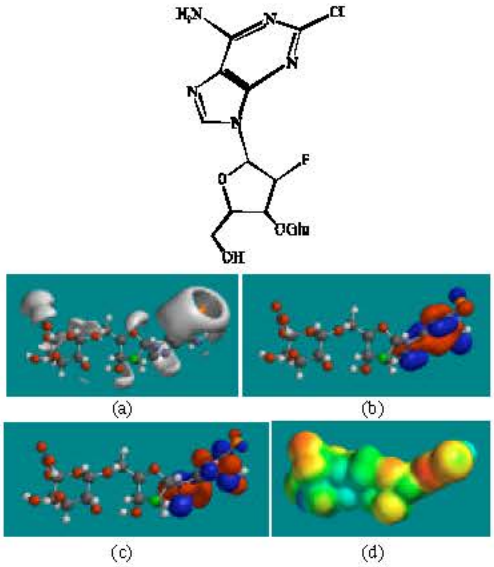

Fig. 5: Structure of CLFG1 giving in: (a) the electrostatic potential (greyish envelope denotes negative electrostatic potential), (b) the HOMOs, (where red indicates HOMOs with high electron density), (c) the LUMOs (where blue indicates LUMOs) and in (d) density of electrostatic potential on the molecular surface (where red indicates negative, blue indicates positive and green indicates neutral)

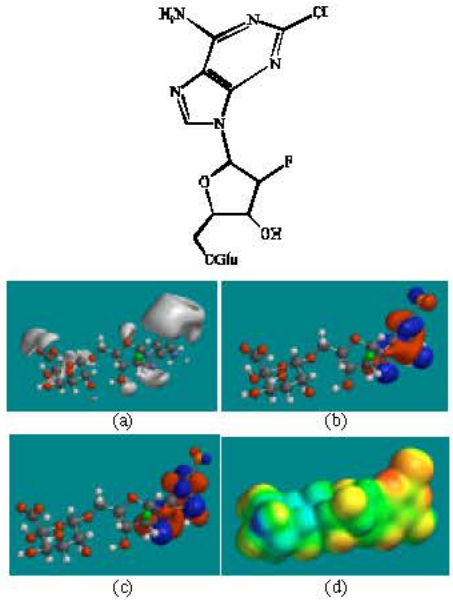

Fig. 6:Structure of CLFG2 giving in: (a) the electrostatic potential (greyish envelope denotes negative electrostatic potential), (b) the HOMOs, (where red indicates HOMOs with high electron density), (c) the LUMOs (where blue indicates LUMOs) and in (d) density of electrostatic potential on the molecular surface (where red indicates negative, blue indicates positive and green indicates neutral)

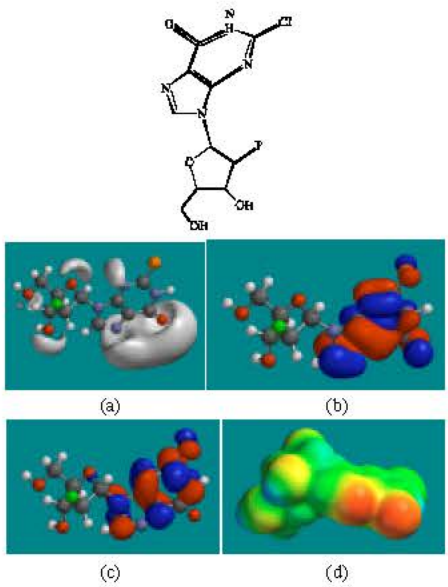

Fig. 7: Structure of 6KCLF giving in: (a) the electrostatic potential (greyish envelope denotes negative electrostatic potential), (b) the HOMOs, (where red indicates HOMOs with high electron density), (c) the LUMOs (where blue indicates LUMOs) and in (d) density of electrostatic potential on the molecular surface (where red indicates negative, blue indicates positive and green indicates neutral)

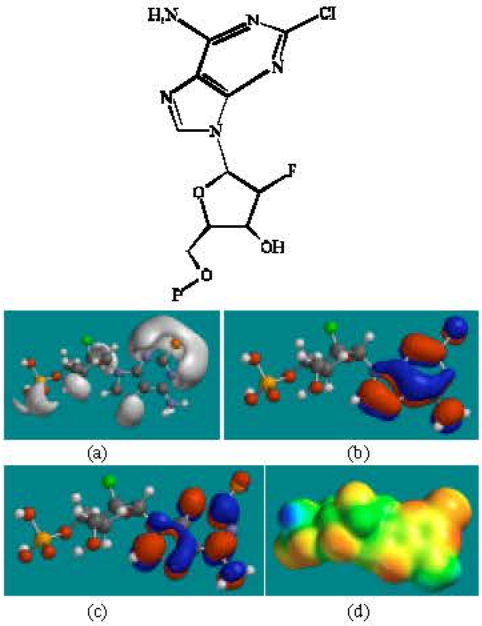

Fig. 8:Structure of CLFMP giving in: (a) the electrostatic potential (greyish envelope denotes negative electrostatic potential), (b) the HOMOs, (where red indicates HOMOs with high electron density), (c) the LUMOs (where blue indicates LUMOs) and in (d) density of electrostatic potential on the molecular surface (where red indicates negative, blue indicates positive and green indicates neutral)

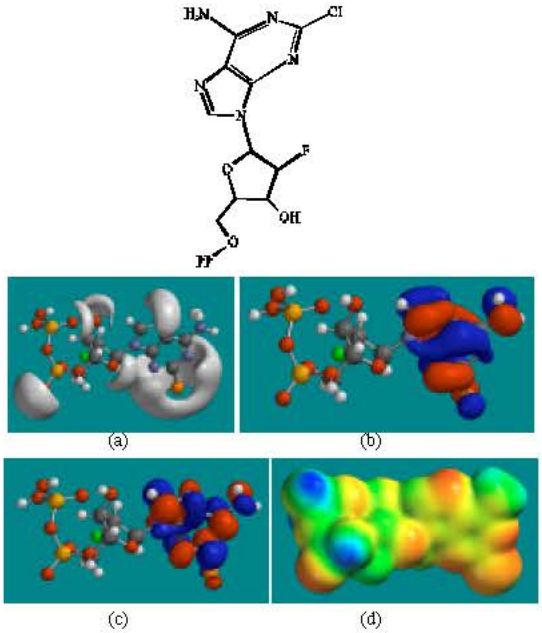

Fig. 9: Structure of CLFDP giving in: (a) the electrostatic potential (greyish envelope denotes negative electrostatic potential), (b) the HOMOs, (where red indicates HOMOs with high electron density), (c) the LUMOs (where blue indicates LUMOs) and in (d) density of electrostatic potential on the molecular surface (where red indicates negative, blue indicates positive and green indicates neutral)

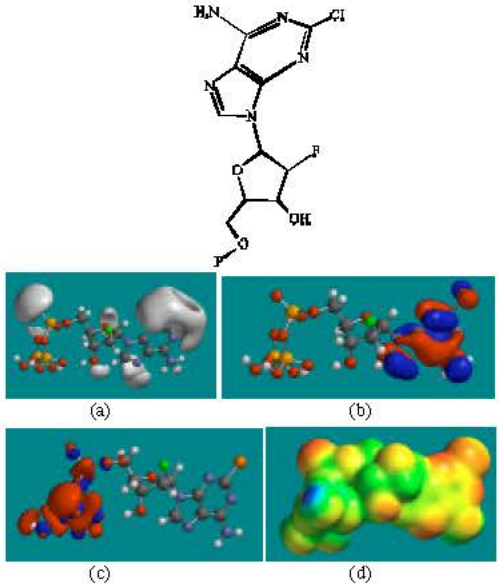

Fig. 10: Structure of CLFTP giving in: (a) the electrostatic potential (greyish envelope denotes negative electrostatic potential), (b) the HOMOs, (where red indicates HOMOs with high electron density), (c) the LUMOs (where blue indicates LUMOs) and in (d) density of electrostatic potential on the molecular surface (where red indicates negative, blue indicates positive and green indicates neutral)

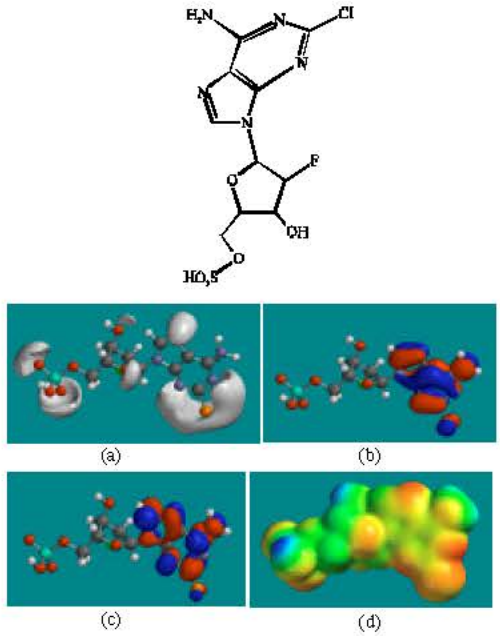

Fig. 11: Structure of CLFS1 giving in: (a) the electrostatic potential (greyish envelope denotes negative electrostatic potential), (b) the HOMOs, (where red indicates HOMOs with high electron density), (c) the LUMOs (where blue indicates LUMOs) and in (d) density of electrostatic potential on the molecular surface (where red indicates negative, blue indicates positive and green indicates neutral)

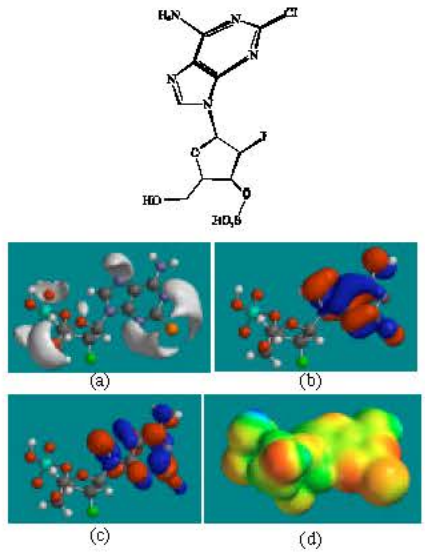

Fig. 12: Structure of CLFS2 giving in: (a) the electrostatic potential (greyish envelope denotes negative electrostatic potential), (b) the HOMOs, (where red indicates HOMOs with high electron density), (c) the LUMOs (where blue indicates LUMOs) and in (d) density of electrostatic potential on the molecular surface (where red indicates negative, blue indicates positive and green indicates neutral)

In the case of CLF, CCLF, CLFG1, CLFG2, 6KCLF, CLFS1 and CLFS2, the electrostatic potential is found to be more negative around Cl, F, N and O atoms, indicating that the positions may be likely to be subject to electrophilic attack. In the case of 2CAD, the electrostatic potential is found to be more negative around Cl and N atoms, indicating that the positions may be subject to electrophilic attack. In the case of CLFMP, CLFDP and CLFTP, the electrostatic potential is found to be more negative around Cl, F, N, P and O atoms, indicating that the positions may be subject to electrophilic attack.

In the case of CLF, CCLF, 2CAD, CLFMP, CLFDP, CLFS1 and CLFS2, both the HOMOs with high electron density and the LUMOs are found to be centered on the non-hydrogen atoms of the adenine rings. In the case of CLFG1, CLFG2 and 6KCLF, both the HOMOs with high electron density and the LUMOs are found to be centered mostly on the non-hydrogen atoms of the purine ring. In the case of the active metabolite CLFTP, the HOMOs with high electron density are found to be centered on the non-hydrogen atoms of the phosphate groups whereas the LUMOs are centered on the non-hydrogen atoms of the adenine moiety. Thus, the active metabolite is uniquely different from CLF and other metabolites in having HOMOs with high electron density and the LUMOs at different locations. It may also be noted CLFTP differs from CLF and all other metabolites in having distinctly different values for surface and volume (Table 1). These differences between CLFTP and the parent drug and other metabolites may be critical in interaction with DNA and binding with DNA polymerase α and ribonucleotide reductase.

The molecular surfaces of CLF and all its metabolites are found to abound in electron-rich (yellow and red) and neutral (green) regions so that the compounds may be subject to electrophilic and lyophilic attacks but the absence of any significant amount of electron-deficient (blue) regions means that the compounds may not be subject to nucleophilic attacks such as those by cellular glutathione and nucleobases in DNA (although the possibility cannot be ignored especially in the case of CLF, 2CAD and CLFDP) so that the compounds generally may not react to any significant extent with cellular nucleophiles such as the reduced form of glutathione and nucleobases in DNA. This means that other factors besides glutathione depletion and DNA damage may be playing key role in toxicity of CLF and its metabolites.

CONCLUSIONS

Clofarabine (CLF) is a new purine nucleoside antimetabolite developed for the treatment of solid and hematologic tumours. Molecular modelling analyses based on molecular mechanics, semi-empirical (PM3) and DFT (at B3LYP/6-31G* level) calculations showed that CLF and all its metabolites have large LUMO-HOMO energy differences so that the compounds would be kinetically inert. The molecular surfaces of CLF and its metabolites are found to abound in electron-rich (red and yellow) and neutral (green) regions so that the compounds may be subject to electrophilic and lyophilic attacks. The absence of any significant amount of electron-deficient (blue) regions means that the compounds may not be subject to nucleophilic attacks such as those by cellular glutathione and nucleobases in DNA (although the possibility cannot be ignored especially in the case of CLF, 2CAD and CLFDP). This means that other factors besides glutathione depletion and DNA damage may be playing key role in toxicity of CLF and its metabolites.

ACKNOWLEDGMENT

Fazlul Huq is grateful to the Discipline of Biomedical Science, School of Medical Sciences, The University of Sydney for the time release from teaching.

REFERENCES

Beonate, P.L., L. Arthaud, J. Stuhler, P. Yerino, R.J. Press and J.Q. Rose, 2005. The distribution, metabolism and elimination of clofarabine in rats. Drug Metab. Dispos., 33: 739-748.

Faderi, S., V. Gandhi, S. O'Brien, P. Beonate, J. Cortes, E. Estey, M. Beran and W. Wierda *et al.*, 2005. Results of phase 1-2 study of clofarabine in combination with ctarabine (ara-C) in relapsed and refractory acute leukemias. Blood, 105: 940-947.

Hegde, S. and M. Schmidt, 2006. Annual Reports in Medicinal Chemistry. Wood, A. (Ed.), 41: 439-477.

Huq, F. and A. Alshehri, 2006. Molecular modelling analysis of the metabolism of diclofenac. Int. J. Pure Applied Chem., 1: 359-373.

Huq, F., 2006a. Molecular modelling analysis of the metabolism of tamoxifen. Int. J. Pure Applied Chem., 1: 155-163.

Huq, F., 2006b. Molecular modelling analysis of the metabolism of zaleplon. J. Pharmacol. Toxicol., 1: 328-336.

Parker, W.B., S.C. Shaddix, C.H. Chang, E.L. White, L.M. Rose and R.W. Brockman *et al.*, 1991. Effects of 2-chloro-90(2-deoxy-2-fluoro-β-D-arabinofuranosyl)adenine on K562 cellular metabolism and the inhibition of human ribonucleotide reductase and DNA polymerases by its 5'-triphosphate. Cancer Res., 51: 2386-2394.

Plunkett, W. and V. Gandhi, 2001. Purine and Pyrimidine Nucleoside Analogs. In: Cancer Chemotherapy and Biologic Response Modifiers. Giaccone, G., R. Schilsky and P. Sondel (Eds.), Annual 19, Elsevier Science, BV, Amsterdam. The Netherlands, pp: 21-45.

Spartan '02, Wavefunction, Inc. Irvine, CA, USA., 2002.

Xie, K.C. and W. Plunkett, 1996. Deoxynucleotide pool depletion and sustained inhibition of ribonucleotide reductase and DNA synthesis after treatment of human lymphoblastoid cells with 2-chloro-9-(2-deoxy-2-fluoro-β-D-arabinofuranosyl)adenine. Cancer Res., 56: 3030-3037.